

Eco-friendly production of metal nanoparticles immobilised on organic monolith for pepsin extraction

Eman Alzahrani*, Ashwaq T. Alkhudaiby

Chemistry Department, Faculty of Science, Taif University, Taif, Kingdom of Saudi Arabia

*Corresponding authors: e-mail: em-s-z@hotmail.com

Polymer monoliths modified by using nanoparticles (NPs) integrate high NP specific surface area with different monolith surface chemistry and high porosity. As a result, they have extensive applications within different fields, whereas nanomaterial-functionalised porous polymer monoliths have elicited considerable interest from investigators. This study is aimed at fabricating organic polymer-based monoliths from polybutyl methacrylate-*co*-ethylenedimethacrylate (BuMA-*co*-EDMA) monoliths prior to immobilization of gold or silver metal on the pore surface of the monoliths using reducing reagent (extracts of lemon peels). This was intended to denote a sustainable technique of immobilizing nanoparticles that are advantageous over physical and chemical techniques because it is safe in terms of handling, readily available, environmentally friendly, and cheap. Two different methods were used in the study to effectively immobilize nanoparticles on monolithic components. The outcomes showed that soaking the monolith rod in the prepared nano solution directly and placing it within ovens at temperatures of 80°C constituted the most effective method. Characterisation of the fabricated monolith was undertaken using SEM/EDX analysis, UV-vis. spectra analysis, and visual observation. The SEM analysis showed that nanoparticles were extensively immobilised on the surface polymers. Another peak was attained through EDX analysis, thus confirming the Au atom existence at 2.83% alongside another peak that proved the Ag atom existence at 1.92%. The fabricated components were used as sorbents for purifying protein. The ideal performance was achieved using gold nanoparticles (GNPs) immobilised organic monolith that attained a greater pepsin extraction recovery compared to silver nanoparticles (SNPs) immobilised organic monoliths alongside bare organic-based monolith.

Keywords: polymer monolith, immobilization, metal nanoparticles, pepsin purification

INTRODUCTION

Monolithic static phases within electrochromatography and chromatography began eliciting the interest of investigators during the 1930s¹⁻³. Such components became popular as they were created from one piece of porous component that feature large flows via pores allowing separations at high rates of flow attained at low backpressures. Monoliths could be derived from organic², inorganic^{4, 5}, and hybrid organic-inorganic materials⁶⁻⁸.

Organic monoliths are characterized by chemical stabilities at an extensive pH range level. Preparing organic monoliths can be considered simple. They could be produced through one-step polymerisation reaction or a common protocol could be utilized for obtaining parent polymers, which is chemically improved without considerably changing morphologies^{8, 9}. Preparation of monolithic columns has been undertaken directly within the confines of polypropylene tubes⁹, poly(ether-etherketone) (PEEK)^{10, 11}, fused silica lined stainless steel¹²⁻¹⁴, fused silica^{1, 2, 15}, and stainless steel¹⁶.

Characterisation of NPs is based on the high surface-to-volume ratio¹⁷; therefore, they may also be utilised for increasing the polymeric monolithic columns surface area¹⁸. Additionally, nano-architectures can be used for introducing more surface functionalities to columns of polymeric monoliths^{8, 18, 19}. Moreover, monolithic adsorbent electrical conductivity, chemical and thermal stabilities, and structural rigidity are easily altered using NPs to increase molecular interactions and other properties²⁰⁻²². Besides, nanoparticles can extend the specific monolith adsorbent surface area for increase of test analyst retention that results in overall reactivity and enhanced selectivity within the adsorbent^{22, 23}.

Improvement of polymers has the potential of resulting in considerable increments in performance. Improved monoliths are characterized by high column effectiveness, good stability, and large surface area. Addition of nanomaterials to monoliths offers proper mechanical stability. Different nanoparticles have been included into polymeric monoliths to regulate monolithic column selectivity and retention characteristics, and in turn modify separation of tiny molecules. The distinct surface properties of nanoparticles alongside their huge surface-to-volume ratio enable the preparation of static phases with unique retentive power, and later increased separation selectivity to achiral and chiral solutes²⁴⁻²⁶. Currently, various methods are employed for modifying nanoparticle monoliths they include attachment of nanoparticles to preformed monolith surfaces, copolymerizing functionalised monomer nanoparticles, and embedding nanoparticles within the monolithic matrices. Even though copolymerization and embedding constitute direct and simplest methods, they lead to spread of nanoparticles in the entire monolithic matrix and thus most are inaccessible on the pore surfaces for desired interactions²⁷⁻²⁹.

It is common knowledge that green chemistry is advantageous compared to physical and chemical techniques because it is safe in terms of handling, readily available, environmentally friendly, and cheap³⁰. The objective for the investigation explored within the paper sought to fabricate organic polymer-based monolith through a poly (BuMA-*co*-EDMA) monolith prior to NPs immobilization (gold and silver) on the monolith surface using extracts of lemon peel as the green technique. Two simple techniques were used to attain the most efficient technique of immobilizing nanoparticles on the monolithic mate-

rial surface: The initial technique involved addition of monolithic rods to nanoparticle solutions whereas the second technique was undertaken through mixing of a reduction reagent with sources of ion (HAuCl_4 or AgNO_3 solution) prior to adding monolithic rods and putting it within an 80°C oven. Different chemical analytical tools such as UV-vis., EDX, and SEM, were utilized within the study to locate variations on surfaces of polymer monoliths prior to and after nanoparticle immobilisation. Organic monoliths prepared within home-made spin columns were utilized for purifying proteins. Monolithic spin columns that constitute a recent inclusion to SPE products were selected as they can increase the speed of sample preparation and accommodation of negligible specimen volumes. While few studies have cited the application of the method, the outcomes thus far can be considered promising³¹.

EXPERIMENTAL

Chemicals and materials

Chloroauric acid 99.9% ($\text{HAuCl}_4 \cdot 3\text{H}_2\text{O}$), silver nitrate 99.8% (AgNO_3), butyl methacrylate 99% (BuMA), ethylene dimethacrylate 98% (EDMA), benzophenone, pepsin from gastric mucosa, and Whatman filter paper (pore size $25 \mu\text{m}$ and diameter 15 cm) were purchased from Sigma Aldrich (Poole, UK). Acetone, trifluoroacetic acid (TFA), acetonitrile (ACN), 1-decanol, methanol, isopropanol and ammonium acetate buffer were purchased from Fisher Scientific (Loughborough, UK). Disposable plastic syringes (1 ml) were purchased from Scientific Laboratory Supplies (Nottingham, UK). Blu-tack was purchased from Bookstore (Taif, KSA). Lemon was collected from a local market (Taif, KSA) and distilled water was used for the preparation purpose.

Instrumentation

A hot-plate stirrer from VWR International LLC (Welwyn Garden City, UK), a UV-vis. spectrophotometer from Thermo Scientific™ GENESYS 10S (Toronto, Canada). The oven came from F.LLI GALLI Company (Milano, Italy). Energy dispersive X-ray (EDX) analysis was performed using an INCA 350 EDX system from Oxford Instruments (Abingdon, UK), and centrifuge was from Lab Essentials, Inc. (Monroe, Georgia, US). Transmission electron microscopy (TEM) from JEOL Ltd. (Welwyn Garden City, UK). A sonicator from Ultrawave Sonicator U 300HD (Cardiff, UK) and UV lamp (365 nm) from Spectronic Analytical Instruments (Leeds, UK) were used the UV-vis. A scanning electron microscope (SEM) Cambridge S360 from Cambridge Instruments (Cambridge, UK) was used. High-resolution atomic force microscopy (AFM) was used to test morphological features and to produce a topological map (Veeco-di Innova Model-2009-AFM-USA). HPLC analysis was carried out using a Perkin Elmer LC200 series binary pump, a Symmetry C_8 column, $4.6 \text{ mm} \times 250 \text{ mm}$ packed with silica particles (size $5 \mu\text{m}$) from Thermo Fisher Scientific (Loughborough, UK) and a Perkin Elmer 785A UV/Visible Detector from Perkin Elmer (California, USA).

Fabrication of monolithic materials

Preparation of polymer-driven monolith in homemade spin columns in room temperature under ultraviolet radiation was achieved through the photo-initiated free radical polymerization. The preparation of polymer-based monoliths was undertaken through the process highlighted in the previous work³² {Alwael, 2011 #289; Alzahrani, 2012 #751} alongside some improvements. The polymerization mix featured the porogenic solvent system ($1450 \mu\text{l}$ of 1-decanol and $4550 \mu\text{l}$ of isopropanol), the free radical photoinitiator (0.1 g of benzophenone), a crosslinker ($1600 \mu\text{l}$ of EDMA), and a monovinyl monomer ($2400 \mu\text{l}$ of BuMA). Sonication of the polymerisation mixture was undertaken for 5 min to dissolve the initiator s and generate a homogeneous solution through a sonicator. A 0.25 ml Eppendorf tube was filled with the polymerisation mix and placed below the ultraviolet lamp at 365 nm in room temperature. After the polymerisation reactions, the monolithic components were washed in distilled water and methanol in the ratio of 50:50.

Immobilisation of nps on the monolith

Two diverse techniques were utilized within the study to locate the optimum method for nanoparticle immobilisation on the polymer monolith surface. The two methods mainly involved soaking monolithic rods (1 cm) within nanoparticle solutions and placing them in 80°C oven. A green chemistry technique to preparing NPs was used with extracts of lemon peel, as stated earlier³³ alongside minor modifications: 20 g of lemon peel were added to 100 ml of deionized water prior to boiling the mixture for 30 min at 80°C . The solution underwent filtration with Whatman paper then added to 2 mM ion source solutions in the ratio of 2:1 at room temperatures ($25 \pm 3^\circ\text{C}$) and preserved within a dark room for 1 day.

Method one. A solution of nanoparticle, prepared 24 h in advance, was put a test tubes. Then, 1 cm monolithic rod was incorporated to the suspension. Finally, the test tubes were placed in oven at temperatures of 80°C for a 5-day period.

Method two. A mix of reducing reagent suspension alongside solution of AgNO_3 or HAuCl_4 in the ratio of 1:2 was put in test tubes. Afterwards, a monolithic rod of 1cm was incorporated to the suspension. Finally, the test tubes were placed in oven at temperatures of 80°C for a 5-day period.

Monolithic material characterisation

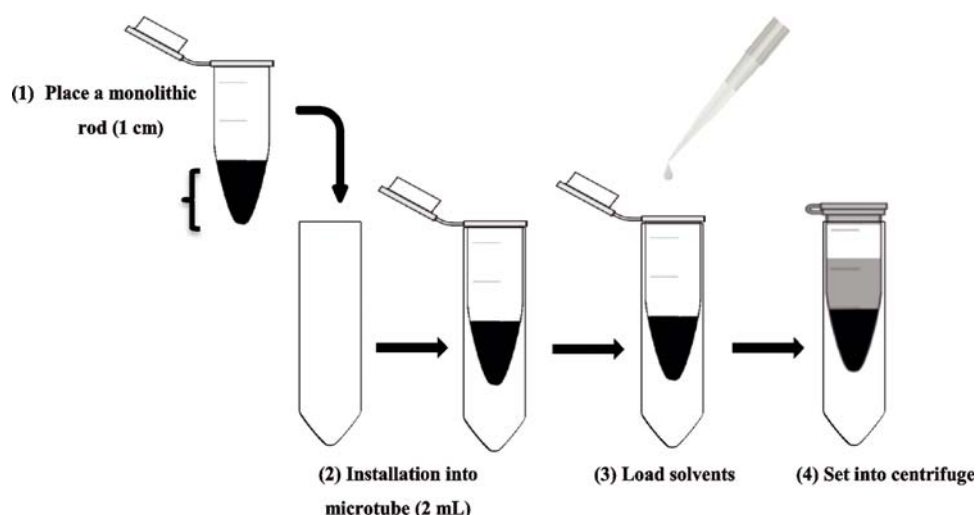
Visual observation and UV-vis. spectra analysis. The ion reduction into nanoparticles is mainly accompanied by a visible change in colour and NPs formation³⁴. In view of this, the colour was observed to determine NP formation. The absorption of the resultant solutions was tracked through UV-vis. spectrophotometrically on the ranges of 350–800 nm at 1 nm in terms of resolution.

SEM-TEM-EDX-AFM analysis. The morphologies for dried monoliths were classified through scanning electron microscopy (SEM). Images were realized with an increasing voltage of 20 kV alongside a probe current of 100 pA under high vacuum modes. The size of nanoparticles was measured using transmission electron microscopy (TEM). For this, $5 \mu\text{L}$ of the sample solu-

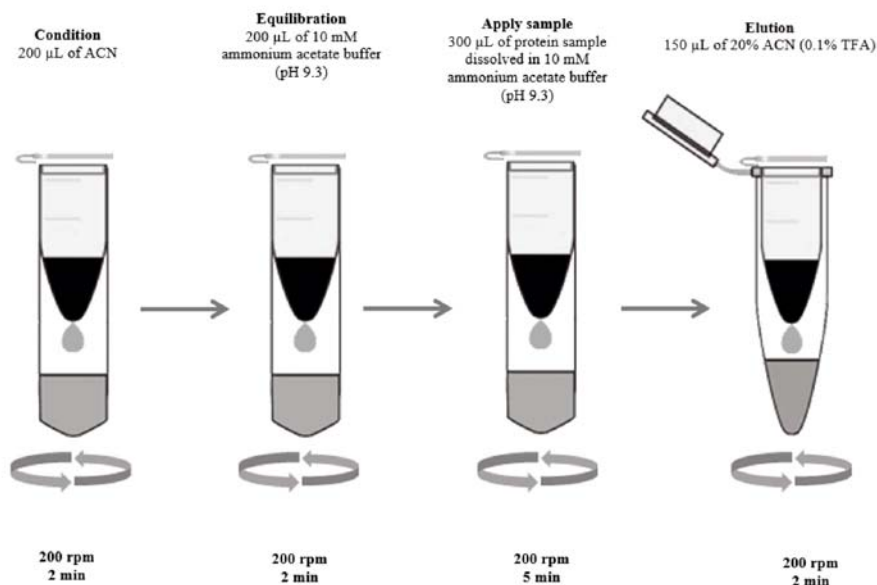
tion was put onto lacy carbon coated 3 mm diameter copper grids. TEM images were acquired with a Gatan Ultrascan 4000 digital camera attached to a JEOL 2010 transmission electron microscope running at 20 kV. The chemical composition of the monolithic components prior to and after the modification of the monolith surface was analyzed using Energy dispersive X-ray (EDX). High-resolution atomic force microscopy (AFM) was employed for testing the topological and morphological characteristics (Veeco-di Innova Model-2009-AFM-USA). Tapping non-contacting modes were utilised. For accurate mapping of surface topologies, AFM-raw data was placed onto the Origin-Lab version 6-USA program to produce accurate visualizations of the 3D surfaces of the samples under study.

Protein extraction

The organic monoliths were put in Eppendorf tubes (0.5 ml) as home-spin columns. The monolith preparation in spin was undertaken using Nakamoto et al.³⁵ method with some few modifications. Scheme 1 recaps the steps used for loading monolithic components within the homemade spin columns.



Scheme 1. Steps of loading monolithic materials in home-made spin column using a centrifuge



Scheme 2. Summary of the handling procedures for protein purification with assist of centrifuge

After the stationary phase, organic monolithic underwent fabrication and its performance verified with pepsin. The protein (60 μM) was immersed in a buffer suspension of 10 mM ammonium acetate (pH 9.3). All experiments were conducted at ambient temperature of about 23°C. Separation of the protein specimen and the solutions was done using the centrifuge at velocities of 200 rpm at a duration of 2-minutes for all steps save for the use of the specimen step that took 5 min. To compute the extraction efficiency of all proteins, individual extraction of the proteins was undertaken. The organic polymeric monoliths underwent activation with 20 μL of acetonitrile (ACN), whereas the solvent was dismissed. Later, it was equilibrated using 200 μL of 10 mM ammonium acetate buffer suspension (pH 9.3), which was rejected. 300 μL made of the protein specimen was loaded and, the elution conducted using 150 μL 20% ACN with 0.1% trifluoroacetic acid (TFA), centrifuged, and then gathered in Eppendorf tubes (1.5 ml). Scheme 2 summarizes the steps that feature in the purification of protein using the fabricated immobilised organic monolith metal NPs.

A specimen of the eluent was placed directly into the HPLC-UV detector to determine the proteins peak point and contrast them to the peak points of protein

standard suspensions to compute the extraction efficiency. The mobile stage constituted acetonitrile-water (50:50) within the existence of 0.1% trifluoroacetic acid (TFA) in isocratic conditions. The wavelength of the detection was modified to 210 nm, whereas the injection volume was 20 ml³⁶. To assess the efficiency of protein extraction, the extraction recovery (ϵ) was computed with equation (1)³⁷⁻³⁹ that was considered the overall protein percentage obtained from the eluent:

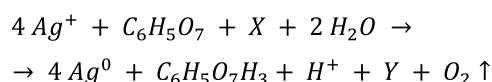
$$ER = \left[\frac{C_{elu} \times V_{elu}}{C_0 \times V_0} \right] \times 100 \quad (1)$$

where C_{elu} and C_0 were derived from the peak point using the solid phase extraction and in the absence of purification, and V_{elu} and V_0 constitute the eluent volumes and solution of the sample.

RESULTS AND DISCUSSION

NPs immobilisation on organic polymer monoliths. Polymer monoliths improved using nanoparticles (NPs) integrate high specific NP surface area properties with the monoliths' different surface chemistry and high porosity. In view of this, they have discovered extensive use in different fields that include sample treatment, electrocatalysis, and chromatography. Notably, nano-material-functionalized porous polymer monoliths have drawn significant attention from investigators^{40, 41}. In the current study, a methacrylate-based monolith (BuMA-co-EDMA) was selected for the organic polymer-based monolith because this was extensively used⁴².

The lemon extract is a source of citric acid, ascorbic acid, and mineral^{43, 44}. Moreover, it contains phytonutrients (phenolic compounds, flavonones-hesperidin, and eriocitrin)⁴⁵. The main indigents in the lemon extract are responsible for a reduction effect is citric acid. The mechanism of formation of silver or gold nanoparticles because of the reduction of metal ions by citric acid can be written as follows:



Where X is unknown bio-organic compounds and on reducing silver ions gets itself oxidized to product(s) Y . We can consider the main reducing reagent in the lemon extract is citric acid as well as some bio-organics⁴⁶.

In this study, the optimised synthesized NPs were characterized using TEM, which can provide information about the size of fabricated nanoparticles. Fig. 1 shows the size distribution histogram of the biofabricated NPs. It was found that the average diameter of the metal nanoparticles was in the range of 44.69 nm.

Monolithic rods underwent coating with nanoparticles two different approaches. The first featured the insertion of organic monolithic rods within NP solutions prior to placement within an 80°C oven. The second involved a mix of reducing reagents using $AgNO_3$ suspension as the source of silver or $HAuCl_4$ suspension as the source of gold followed by addition of monolithic rods prior to placement in test tube in an 80°C oven. Any change in the solutions colour was observed with naked eyes, as illustrated in Fig. 2. The nanoparticle suspension solution that was SNPs suspension solution (Fig. 2a), or GNPs

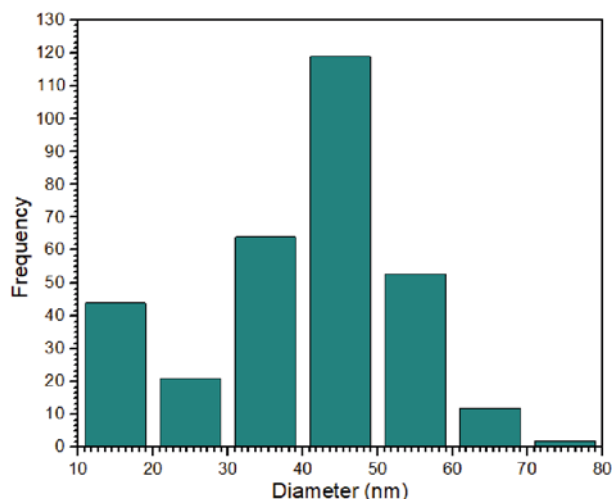


Figure 1. Particle size distribution histogram of metal nanoparticles prepared from lemon peel extract

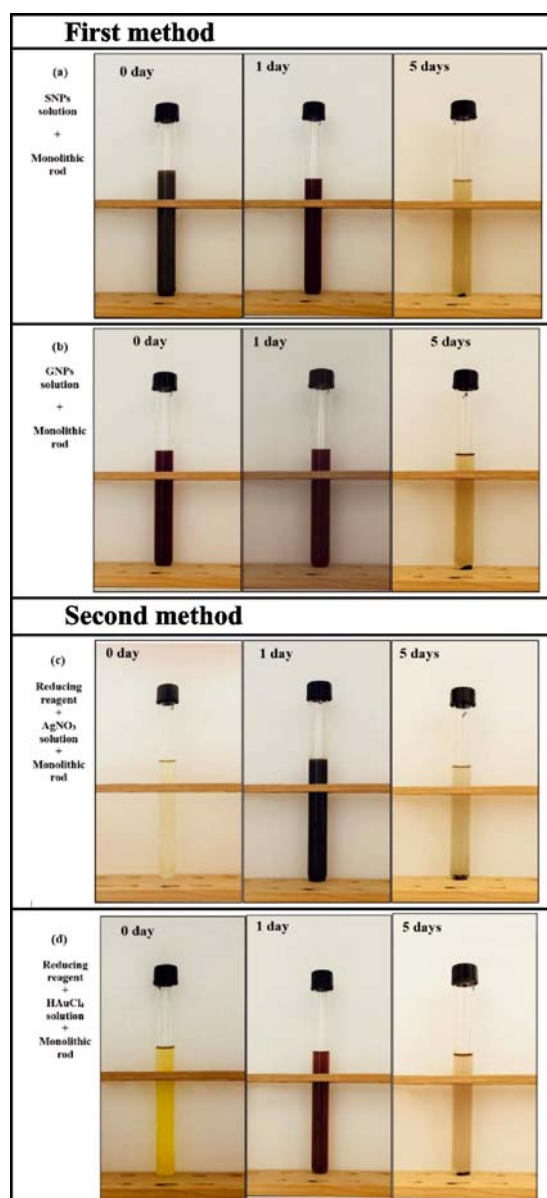


Figure 2. Coating of organic monolithic rods with NPs using the first and second methods (the first method involved placing the monolithic rod in SNPs suspension (a) and GNPs suspension (b), while the second method involved placing the monolithic rod in a mixture of ion source solution ($AgNO_3$ solution (c) or $HAuCl_4$ solution (d)) and reducing reagent (lemon peel extract)

suspension solution (Fig. 2b), was put in test tubes that had the organic monolithic rods. As illustrated, the solution of NPs had a dark colour. After 5 days, the colour intensity of the solution decreased because of the organic monolithic rod nanoparticle coating, whereas the organic monolithic rod colour shifted to dark colour. In the second technique, the source of ion that assumed the form of AgNO_3 solution (Fig. 2c), or a HAuCl_4 solution (Fig. 2d), was mixed using reducing reagent and put in test tubes, which contained organic monolithic rods. The solution of ion source changed to a darker colour because of metallic NP formation. The colour intensity then reduced as the metallic nanoparticle coated the monolithic components.

The NP solution absorption spectra was recorded to determine the NP immobilisation progress on the organic monolithic component over 350–800 nm range. Fig. 3a illustrates the SNPs UV-vis. spectra solution prior to and following NP immobilisation on the organic monolithic component. The SNPs solution featured the absorbance peak of about 2.0 a.u., the organic monolithic rods were incorporated to the solution and measurement of the mixture absorbance was taken one day later. The results showed that there was decrease in the absorbance peak with a shift of 1.3 a.u.. After incubation of the organic monolithic rod within the SNP solution for a 5-day period, no additional absorbance was witnessed as the SNPs had shifted to the organic material surface. Fig. 3b illustrates the UV spectrum of the GNPs suspension whereas the peak of absorbance peak was at 1.8 a.u.. The peak of absorbance reduced to 1.47 a.u. and finally vanished after five-day incubation period with the organic monolithic rods.

Figs 3c and d illustrate the solutions spectra after implementation of the second technique. The results show the absence of absorbance peak for the mixture

consists of reducing reagent and the solution of ion source. The progress characterizing the formation of nanoparticles was checked in 1 day mixing the sources of ion with the reducing reagents in organic monolithic rod presence. The UV-vis. spectra indicated the absence of absorption bands due to the NP transverse plasmon resonance. After 5 days, there were no peaks for the formed nanoparticle solution, showing the completion of NPs immobilisation process on polymer monoliths.

Fig. 4 illustrates the organic monolithic rod's surface colour prior to and following NP immobilisation through the first and second techniques. The bare organic-oriented

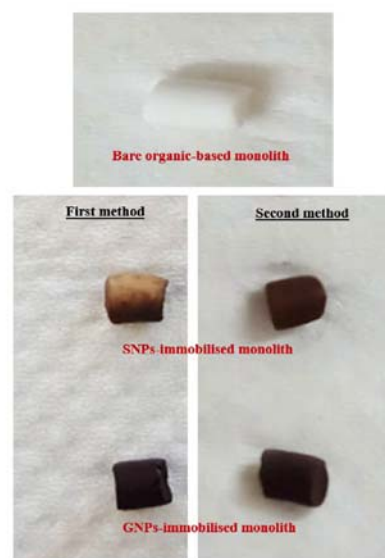


Figure 4. Colour changes of monolith before and after the process of immobilisation of NPs using first and second methods.

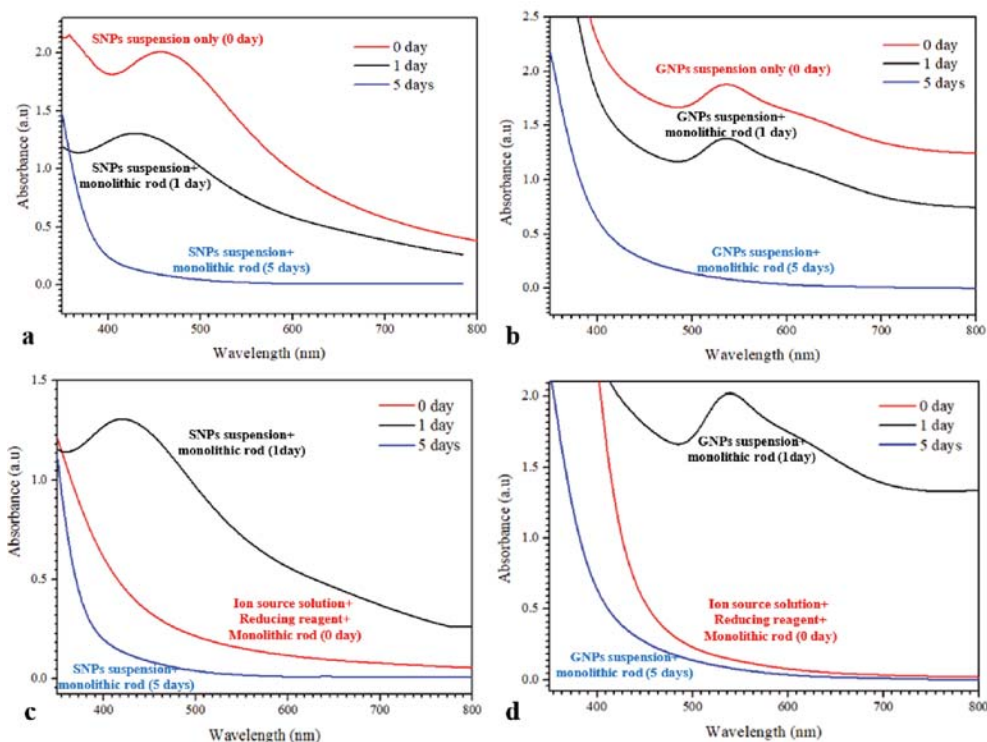


Figure 3. UV-vis. absorption spectra of solution prepared using first and second methods (the first method involved placing the monolithic rod in SNPs suspension (a) and GNPs suspension (b), while the second method involved placing the monolithic rod in a mixture of ion source solution (AgNO_3 solution (c) or HAuCl_4 solution (d)) and reducing reagent (lemon peel extract)

monolith was white. Following NP immobilisation on the monolithic component surface, it changed to a dark colour because of high NP concentration, homogeneous NP distribution, alongside non-cracking. This proved that the nanoparticles had moved to the organic monolithic material surface.

It was imperative to confirm homogeneity on the overall fabricated monolithic component surface area; in view of this, the fabricated organic monolithic rod was separated into three pieces (bottom, middle, top). Fig. 5 illustrates the images of the organic monolith cross-section following the introduction of the NPs using methods one and two. The results showed that GNP immobilisation on the organic monolithic components was better compared to that of SNPs because the internal part of the SNP-immobilised monolith showed lighter colour, while the GNPs-immobilised monolith colour was homogenous and darker. Besides, the second technique seemed to efficiently facilitate NP immobilisation to the organic monolith surface because the monolithic cross section colour (bottom, middle, and top) was homogeneous and darker as opposed to the monolithic components prepared using the first technique.

Characterizations of fabricated materials.

The polymeric monoliths morphologies were examined through SEM analysis, as illustrated in Fig. 6. In general, the surface of all specimens were crack-free, smooth, and uniform, and the porous structure resembled that seen in previous studies^{47, 48}. In addition, it was found

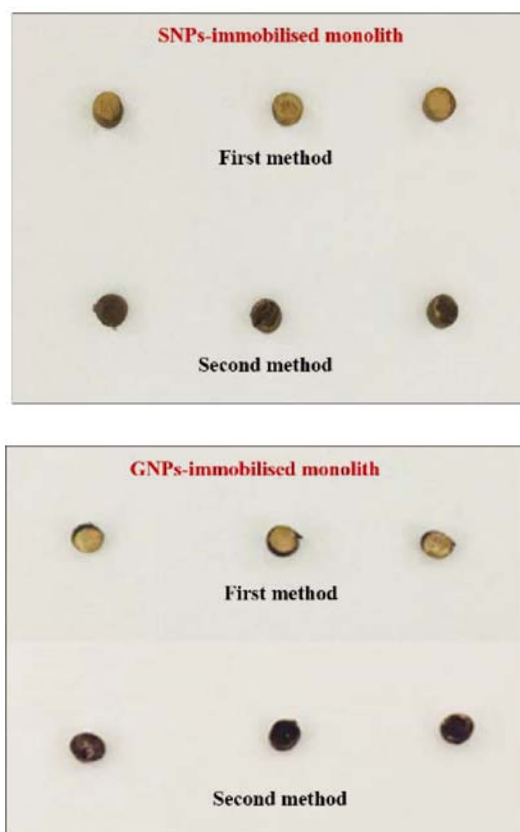


Figure 5. Organic monolithic rod that was divided into three cross-sections (top, middle, and bottom) after immobilisation with NPs

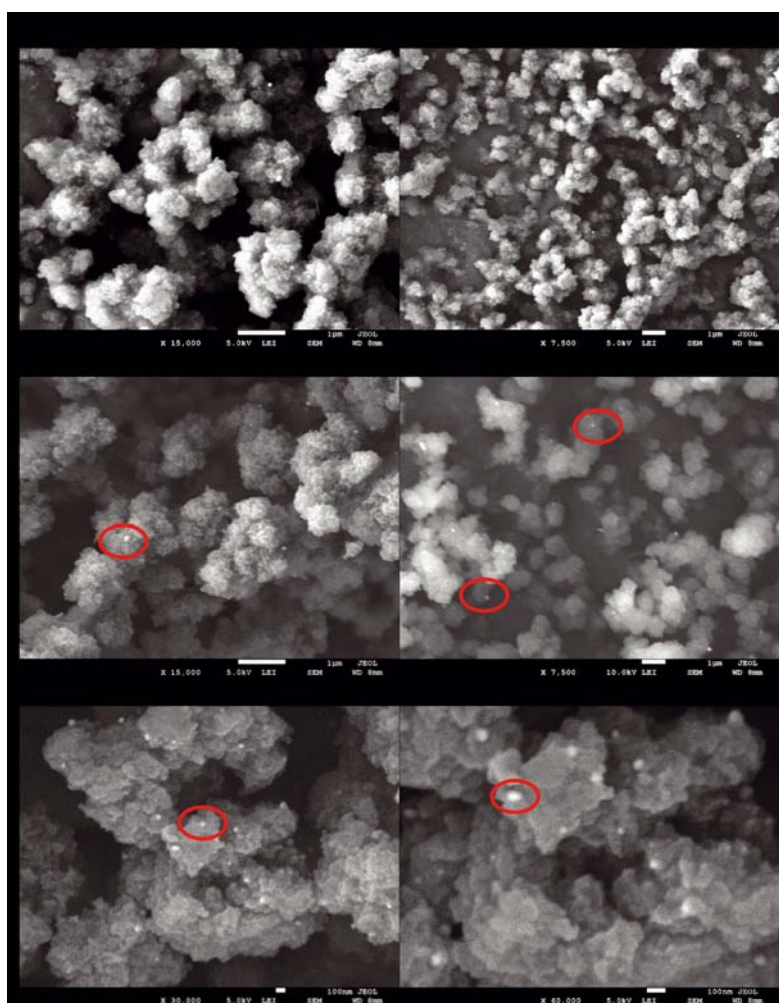


Figure 6. Scanning electron micrographs showing the surface morphology of bare organic monolith, SNPs-immobilised organic monolith, and GNPs-immobilised organic monolith. Modified

that the SEM of bare organic-based monoliths a suitable pore structure was detected that showed a homogeneous interrelated macro-porous network with open pores. The SEM of SNPs-immobilised monolith alongside GNPs-immobilised monolith proved the suitable pore surface coverage with nanoparticles that the nanoparticles had spherical shapes. Similar results were obtained in Refs 50–53. Additionally, the results showed that there were variations in the fabricated monolithic material morphologies coated using NPs irrespective of whether the second or first method was used.

EDX analysis was used for investigating the fabricated monolithic materials chemical composition illustrated in Fig. 7. The results indicated that the major elements of bare organic-based monoliths included oxygen (O) and carbon (C). After the immobilisation of SNPs on the organic monolith surface with the second or first method, besides oxygen and carbon, a new optimal point in Ag was identified, as illustrated by the increasing Ag peak intensity. In the scenario for the first technique, oxygen and carbon peaks were identified with Au pattern showing a new peak. Regarding the second technique, there was increased Au peak intensity.

Table 1 recaps the data relating to the fabricated material chemical composition, which were studied through EDX analysis. The bare organic-based monolith comprised of 37.99% O and 62.01% C. After employing the first technique for SNPs immobilisation, carbon was 85.28%, oxygen was 13.49%, whereas silver was 1.23%. After applying the second technique for organic monolith immobilisation, the SNP organic monoliths, silver was 1.92%, oxygen was 24.35%, and carbon was 73.73%. Employing the first technique for GNP immobilisation on the organic monolithic material surface led to 19.64% oxygen, 79.58% carbon alongside a new peak in gold pattern that had gold atom 0.78%. In contrast, applying the second technique for GNP immobilisation on the organic monolith material surface resulted in new gold pattern peak with gold atom 2.83%, 13.60% oxygen and 83.57% carbon. The EDX analysis results show that the second technique constituted the most efficient technique for NP immobilisation on the organic monolithic material surface.

The surface characteristics of coated metallic NPs were examined through AFM, because AFM investigation offers quantitative and qualitative information regarding the scanned particles height. Table 2 provides 3D AFM images for fabricated polymer monoliths prior to and following immobilisation as derived through the AFM method. The bare monolith flat surface was uniform and smooth whereas the roughness of the surface ranged between 17 and 36 nm. The 3D AFM image of the SNPs immobilisation revealed that the roughness of

the surface increased slightly to 19–38 nm while, after GNP immobilisation to the monolithic component, the roughness of the surface roughness increased and ranged

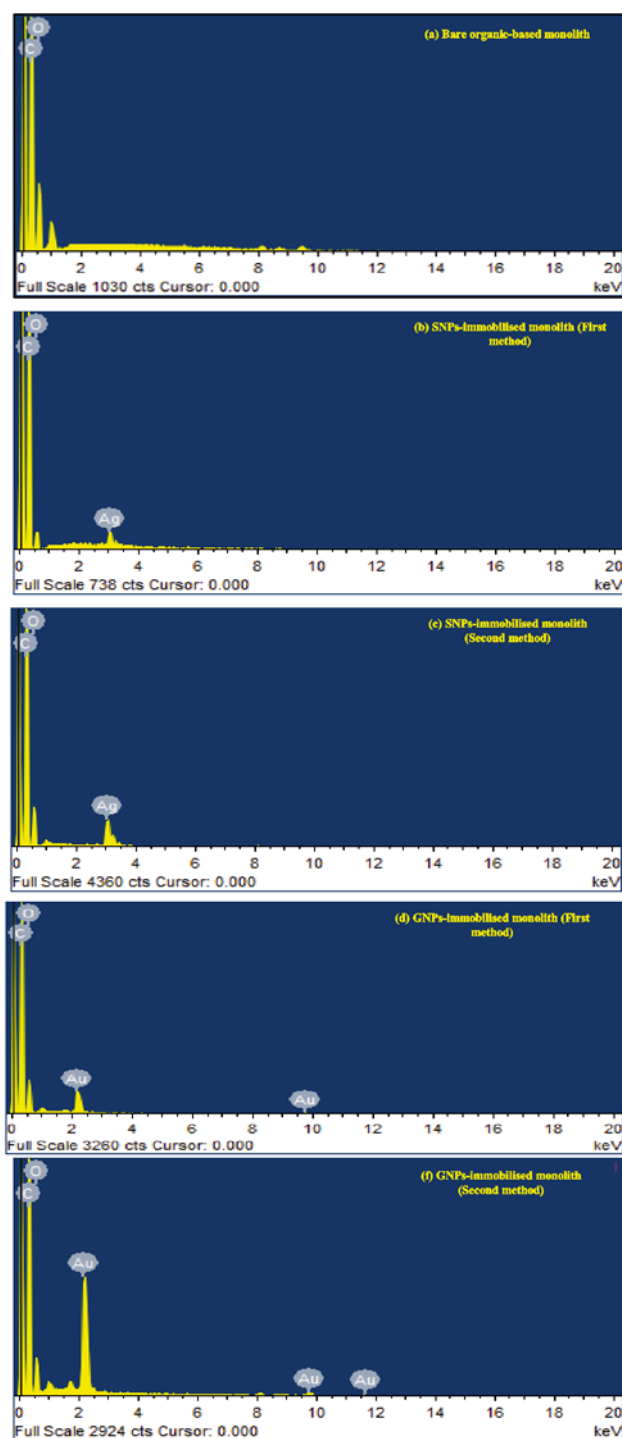
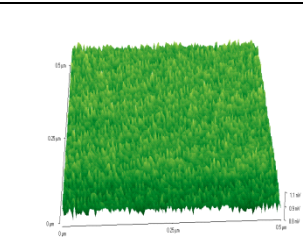
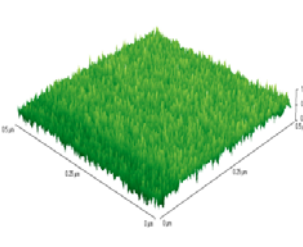
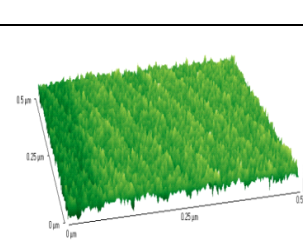


Figure 7. EDX images of the bare organic-based monolith (a), SNPs-immobilised organic monolith using first method (b) and second method (c), and GNPs-immobilised organic monolith using first method (d) second method (e)

Table 1. Composition components of bare organic monolith, SNPs-immobilised organic monolith, and GNPs-immobilised organic monolith

Element	Organic monolith	SNPs-immobilised organic monolith		GNPs-immobilised organic monolith	
		First method	Second method	First method	Second method
C	68.49	85.28	73.73	79.58	83.57
O	31.51	13.49	24.35	19.64	13.60
Ag	00	1.23	1.92	00	00
Au	00	00	00	0.78	2.83
Totals	100.00	100.00	100.00	100.00	100.00

Table 2. Particle size of organic monolith before and after immobilisation of NPs using AFM technique

Type of monolith	3D-AFM-micrograph	Roughness [nm]
Bare organic monolith		17–36
SNPs-immobilised organic monolith		19–38
GNPs-immobilised organic monolith		21–43

between 21 and 43 nm. The 3D AFM results proved the NP immobilisation with organic monoliths. Based upon the classification of fabricated components, it could be inferred that the second method efficiently immobilised NP monolithic materials compared to the first technique; in view of this, the second technique was used for NP monolithic materials.

Performance for protein purification. Sample preparation constitutes a crucial step within analytical protocols. Because of their significant surface-to-volume ratio, nanoparticles have in recent years been considered efficient affinity probes for SPE³⁰. Following monolithic material fabrication (GNPs immobilised organic monolith, SNPs immobilised organic monolith, and bare organic monolith), they were utilized as SPE sorbents for pepsin enrichment (the source being gastric mucosa, 66463 Da, $pI = 4.7$).

Monolithic spin columns, a latest inclusion to SPE products, were chosen for this role as they can accelerate sample preparation velocity and accommodate tiny volumes of samples³¹. The extraction of samples followed four steps as illustrated in the procedure within Scheme 2 that featured protein elution, sorbent equilibration and activation, and sample solution loading through Eman Alzahrani method³² with minor modifications. Firstly, the monolith was activated with 200 μl of ACN, and then equilibrated with 200 μl of 10 mM ammonium acetate buffer solution (pH 9.3), then 300 μl the sample solution were loaded. Finally, the extracted protein was eluted from the fabricated organic polymer monolith using 150 μl of 20% ACN (0.1% TFA) solution as an eluting solu-

tion. All solutions and the protein samples were separated using the centrifuge at speed of 200 rpm within 2 min for all steps except apply sample step takes 5 min.

After preconcentration of the standard protein, the performance of the fabricated polymer monolith was checked using the HPLC-UV detector by comparing the peak area of each protein before and after preconcentration. Fig. 8 shows the UV chromatogram for the eluent solution of pepsin, which shows a comparison of the peaks area of pepsin before preconcentration (a), and after preconcentration using bare organic monolith (b), SNPs-immobilised organic monolith (c), and GNPs-immobilised organic monolith (d). The standard protein investigated for comparison of the performance of bare organic monolith, immobilised monolith with GNPs and immobilised monolith with SNPs. From figure 8 and Table 3 that shows the peak area and peak height of standard pepsin before and after preconcentration, it can be seen that a difference in the peak height and peak area of protein with bare monolith compared with the monolith with NPs. As a result, the sensitivity of the analysis was enhanced, when using monolith immobilised with NPs. In addition, the performance of GNPs immobilised organic monolith was better than that of SNPs immobilised organic monolith.

Table 3. The data relating to peak height and peak area of standard pepsin before and after extraction using the fabricated monolithic materials

	Peak height	Peak area
Standard pepsin (60 μM)	355	69
Preconcentrated pepsin using bare organic-based monolith	761	91
Preconcentrated pepsin using SNPs-immobilised organic monolith	903	100
Preconcentrated pepsin using GNPs-immobilised organic monolith	1190	113

As can be seen in Fig. 9, the extraction recoveries of the standard protein was calculated and it was found that the extraction recovery of pepsin using bare organic-based monolith was 84.6%, which were less than the extraction recoveries of the same proteins using organic monolith coated with NPs. In addition, it was found that the extraction recovery of pepsin using organic monolith coated with GNPs (99.8%) has higher than the extraction recovery of the same protein using organic monolith coated with SNPs (87.5%), and it is similar to other study published in Refs^{50, 53–54}. The results obtained from this investigation showed that the procedure to preconcentrate pepsin was reproducible since good run-to-run reproducibility was achieved with RSD value was less than 5%.

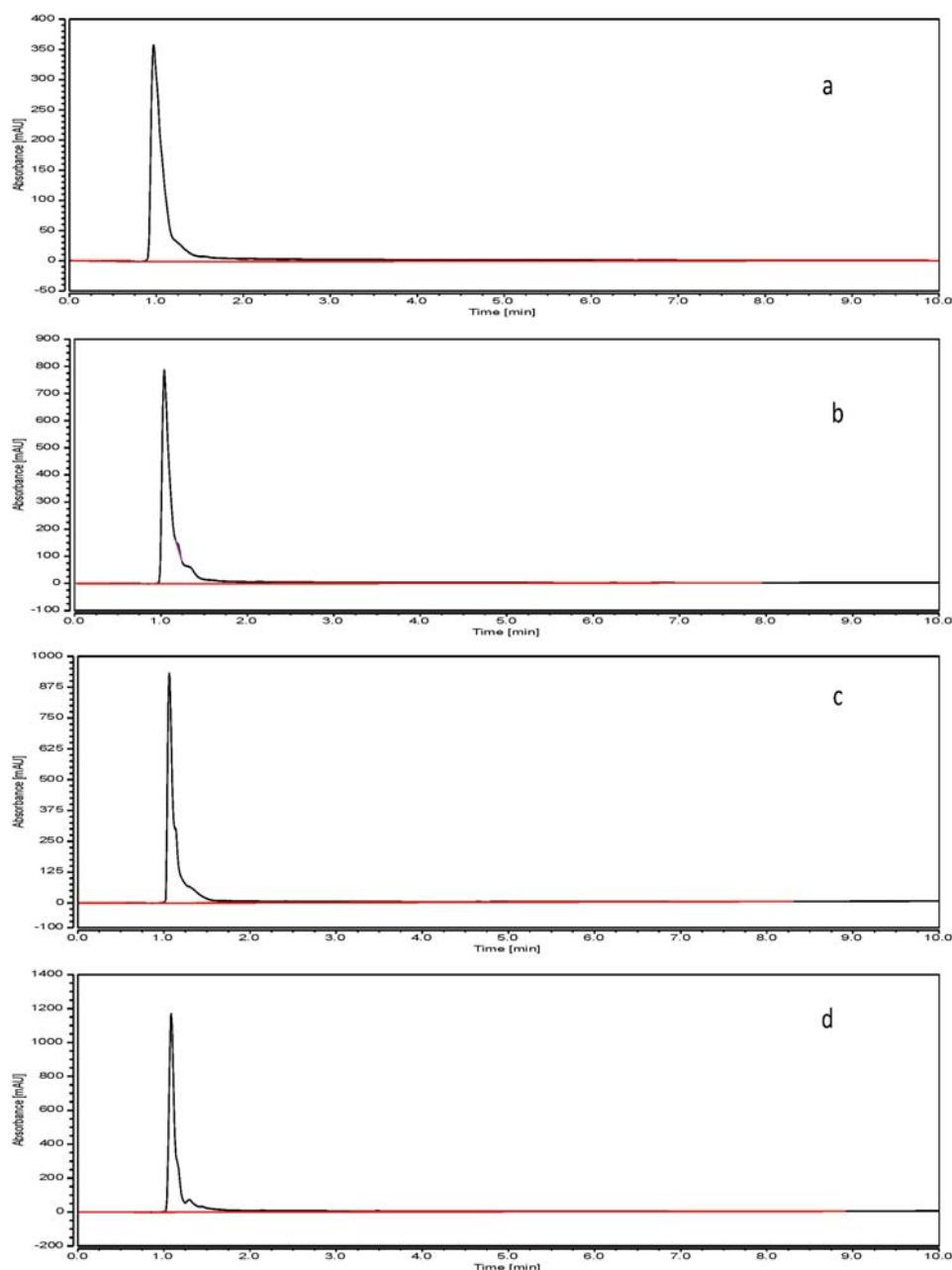


Figure 8. Difference in the peak areas of pepsin before pre-concentration – a, and after pre-concentration using the bare organic-based monolith – b, SNPs-immobilised organic monolith – c, and GNPs-immobilised organic monolith – d

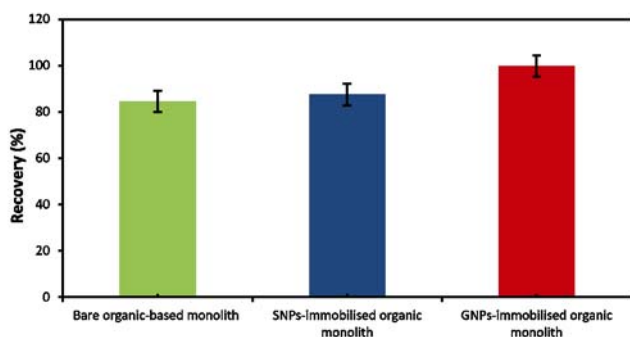


Figure 9. Comparison of the extraction recovery of pepsin using bare organic-based monolith, SNPs-immobilised organic monolith, and GNPs-immobilised organic monolith

CONCLUSIONS

This project sought to fabricate organic monolithic materials within home-made spin columns for application in extraction of protein samples as the means for accessing

the benefits of reduced analysis time, contamination, and specimen handling. The technique tested used green chemistry methods to prepare metal NPs because they were considered environmental-friendly, readily available and safe. Two techniques of NP immobilisation on organic-based monoliths underwent testing during the study, and overall, it was found that the second technique was more efficient compared to the first one for NP immobilisation on monolithic material surfaces. The use of optimized monolithic components in a process of protein extraction was studied. The results showed that organic monoliths modified using NPs had better performance compared to bare organic-based monoliths.

LITERATURE CITED

1. Guiochon, G. (2007). Monolithic columns in high-performance liquid chromatography. *J. Chromatogr. A.* 1168(1–2), 101–168. DOI: 10.1016/j.chroma.2007.05.090.

2. Svec, F. & Huber, C.G. (2006). Monolithic materials: Promises, challenges, achievements. *Anal. Chem.* 78(7), 2100–2107. DOI: 10.1021/ac069383v.
3. Wang, J., Shen, S., Lu, X. & Ye, F. (2017). One-pot preparation of an organic polymer monolith by thiolene click chemistry for capillary electrochromatography. *J. Separ. Sci.* 40(15), 3144–3152. DOI: 10.1002/jssc.201700110.
4. Kabir, A., Furton, K.G. & Malik, A. (2013). Innovations in sol-gel microextraction phases for solvent-free sample preparation in analytical chemistry. *TrAC Trends Anal. Chem.* 45, 197–218. DOI: 10.1016/j.trac.2012.11.014.
5. Zhu, T. & Row, K.H. (2012). Preparation and applications of hybrid organic-inorganic monoliths: a review. *J. Separ. Sci.* 35(10–11), 1294–1302. DOI: 10.1002/jssc.201200084.
6. Alves, F., Scholder, P. & Nischang, I. (2013). Conceptual design of large surface area porous polymeric hybrid media based on polytetrahydrofuran oligomeric silsesquioxane precursors: Preparation, tailoring of porous properties, and internal surface functionalization. *ACS Appl. Mater. Inter.* 5(7), 2517–2526. DOI: 10.1021/am303048y.
7. Svec, F. (2010). Porous polymer monoliths: Amazingly wide variety of techniques enabling their preparation. *J. Chromatogr. A*, 1217(6), 902–924. DOI: 10.1016/j.chroma.2009.09.073.
8. Cao, Q., Xu, Y., Liu, F., Svec, F. & Fréchet, J.M. (2010). Polymer monoliths with exchangeable chemistries: use of gold nanoparticles as intermediate ligands for capillary columns with varying surface functionalities. *Anal. Chem.* 82(17), 7416–7421. DOI: 10.1021/ac1015613.
9. Ishizuka, N., Minakuchi, H., Nakanishi, K., Soga, N., Nagayama, H., Hosoya, K. & Tanaka, N. (2000). Performance of a monolithic silica column in a capillary under pressure-driven and electrodriven conditions. *Anal. Chem.* 72(6), 1275–1280. DOI: 10.1021/ac990942q.
10. Iacono, M., Connolly, D. & Heise, A. (2016). Fabrication of a GMA-co-EDMA monolith in a 2.0 mm id polypropylene housing. *Materials*, 9(4), 263. DOI: 10.3390/ma9040263.
11. Ishizuka, N. (2002). Monolithic silica columns for high-efficiency separations by high-performance liquid chromatography. *J. Chromatogr. A*, 960(1–2), 85–96. DOI: 10.1016/S0021-9673(01)01580-1.
12. Masini, J.C. (2016). Semi-micro reversed-phase liquid chromatography for the separation of alkyl benzenes and proteins exploiting methacrylate- and polystyrene-based monolithic columns. *J. Separ. Sci.* 39(9), 1648–1655. DOI: 10.1002/jssc.201600049.
13. Lv, C., Heiter, J., Haljasorg, T. & Leito, I. (2016). Covalent attachment of polymeric monolith to polyether ether ketone (PEEK) tubing. *Anal. Chim. Acta*, 932, 114–123. DOI: 10.1016/j.aca.2016.05.026.
14. Shu, S., Kobayashi, H., Okubo, M., Sabarudin, A., Butsugan, M. & Umemura, T. (2012). Chemical anchoring of lauryl methacrylate-based reversed phase monolith to 1/16" o.d. polyetheretherketone tubing. *J. Chromatogr. A*, 1242, 59–66. DOI: 10.1016/j.chroma.2012.04.030.
15. Masini, J.C. (2016). Separation of proteins by cation-exchange sequential injection chromatography using a polymeric monolithic column. *Anal. Bioanal. Chem.* 408(5), 1445–1452. DOI: 10.1007/s00216-015-9242-9.
16. Svec, F. & Lv, Y. (2014). Advances and recent trends in the field of monolithic columns for chromatography. *Anal. Chem.* 87(1), 250–273. DOI: 10.1021/ac504059c.
17. Krenkova, J. & Foret, F. (2011). Iron oxide nanoparticle coating of organic polymer-based monolithic columns for phosphopeptide enrichment. *J. Separ. Sci.* 34(16–17), 2106–2112. DOI: 10.1002/jssc.201100256.
18. Currivan, S. & Jandera, P. (2014). Post-polymerization modifications of polymeric monolithic columns: a review. *Chromatogr.* 1(1), 24–53. DOI: 10.3390/chromatography1010024.
19. Zhang, A., Ye, F., Lu, J. & Zhao, S. (2013). Screening α -glucosidase inhibitor from natural products by capillary electrophoresis with immobilised enzyme onto polymer monolith modified by gold nanoparticles. *Food Chem.* 141(3), 1854–1859. DOI: 10.1016/j.foodchem.2013.04.100.
20. Groarke, R.J. & Brabazon, D.B. (2016). Methacrylate polymer monoliths for separation applications. *Materials*, 9(6), 446. DOI: 10.3390/ma9060446.
21. Walsh, Z., Abele, S., Lawless, B., Heger, D., Klán, P., Breadmore, M.C., Paull, B. & Macka, M. (2008). Photoinitiated polymerisation of monolithic stationary phases in polyimide coated capillaries using visible region LEDs. *Chem. Commun.* 48, 6504–6506. DOI: 10.1039/b816958f.
22. Wei, Z.-H., Mul, N., Huang, Y.P. & Liu, Z.S. (2017). Imprinted monoliths: recent significant progress in analysis field. *TrAC Trends Anal. Chem.* 86, 84–92. DOI: 10.1016/j.trac.2016.10.009.
23. Walsh, Z., Levkin, P.A., Abele, S., Scarmagnani, S., Heger, D., Klán, P., Diamond, D., Paull, B., Svec, F. & Macka, M. (2011). Polymerisation and surface modification of methacrylate monoliths in polyimide channels and polyimide coated capillaries using 660 nm light emitting diodes. *J. Chromatogr. A*, 1218(20), 2954–2962. DOI: 10.1016/j.chroma.2011.03.021.
24. Ahmed, M., Yajadda, M.M., Han, Z.J., Su, D., Wang, G., Ostrikov, K.K. & Ghanem, A. (2014). Single-walled carbon nanotube-based polymer monoliths for the enantioselective nano-liquid chromatographic separation of racemic pharmaceuticals. *J. Chromatogr. A*, 1360, 100–109. DOI: 10.1016/j.chroma.2014.07.052.
25. Carrasco-Correa, E.J., Martínez-Vilata, A., Herrero-Martínez, J.M., Parra, J.B., Maya, F., Cerdà, V., Cabello, C.P., Palomino, G.T. & Svec, F. (2017). Incorporation of zeolitic imidazolate framework (ZIF-8)-derived nanoporous carbons in methacrylate polymeric monoliths for capillary electrochromatography. *Talanta*, 164, 348–354. DOI: 10.1016/j.talanta.2016.11.027.
26. Ganewatta, N. & El Rassi, Z. (2018). Monolithic capillary columns consisting of poly (glycidyl methacrylate-co-ethylene glycol dimethacrylate) and their diol derivatives with incorporated hydroxyl functionalized multiwalled carbon nanotubes for reversed-phase capillary electrochromatography. *Analyst*, 143(1), 270–279. DOI: 10.1039/C7AN01426K.
27. Ding, X., Yang, J. & Dong, Y. (2018). Advancements in the preparation of high-performance liquid chromatographic organic polymer monoliths for the separation of small-molecule drugs. *J. Pharmac. Anal.* 8(2), 75–85. DOI: 10.1016/j.jpha.2018.02.001.
28. Hu, W., Hong, T., Gao, X. & Ji, Y. (2014). Applications of nanoparticle-modified stationary phases in capillary electrochromatography. *TrAC Trends in Anal. Chem.* 61, 29–39. DOI: 10.1016/j.trac.2014.05.011.
29. Krenkova, J., Foret, F. & Svec, F. (2012). Less common applications of monoliths: V. Monolithic scaffolds modified with nanostructures for chromatographic separations and tissue engineering. *J. Sep. Sci.* 35(10–11), 1266–1683. DOI: 10.1002/jssc.201100956.
30. Ponarulselvam, S., Panneerselvam, C., Murugan, K., Aarthi, N., Kalimuthu, K. & Thangamani, S. (2012). Synthesis of silver nanoparticles using leaves of *Catharanthus roseus* Linn. G. Don and their antiplasmodial activities. *Asian Pacific J. Tropical Biomed.* 2(7), 574–580. DOI: 10.1016/S2221-1691(12)60100-2.
31. Bunch, D.R. & Wang, S.W. (2013). Applications of monolithic solid-phase extraction in chromatography-based clinical chemistry assays. *Anal. Bioanal. Chem.* 405(10), 3021–3033. DOI: 10.1007/s00216-013-6761-0.
32. Alzahrani, E.S. (2012). Investigation of monolithic materials for protein sample preparation. University of Hull.
33. Aysha, O. & Najimu, S. (2014). Biosynthesis of silver nanoparticles, using Citrus limon (LINN.) Burm. F. Peel extract and its antibacterial property against selected urinary tract pathogens. *J. Bio and Sci., Opi*, 2(3), 248–252. DOI: 10.7897/2321-6328.02355.

34. Alzahrani, E. & Welham, K. (2014). Optimization preparation of the biosynthesis of silver nanoparticles using watermelon and study of its antibacterial activity. *Internat. J. Basic Appl. Sci.* 3(4), 392. DOI: 10.14419/ijbas.v3i4.3358.
35. Nakamoto, A., Nishida, M., Saito, T., Kishiyama, I., Miyazaki, S., Murakami, K., Nagao, M. & Namura, A. (2010). Monolithic silica spin column extraction and simultaneous derivatization of amphetamines and 3, 4-methylenedioxymphetamines in human urine for gas chromatographic-mass spectrometric detection. *Anal. Chim. Acta*, 661(1), 42–46. DOI: 10.1016/j.aca.2009.12.013.
36. Alzahrani, E. & Welham, K. (2011). Design and evaluation of synthetic silica-based monolithic materials in shrinkable tube for efficient protein extraction. *Analyst*, 136(20), 4321–4327. DOI: 10.1039/C1AN15447H.
37. Nagaraju, D. & Huang, S.D. (2007). Determination of triazine herbicides in aqueous samples by dispersive liquid-liquid microextraction with gas chromatography-ion trap mass spectrometry. *J. Chromatogr. A*, 1161(1), 89–97. DOI: 10.1016/j.chroma.2007.05.065.
38. Rezaee, M., Assadi, Y., Milani Hosseini, M.R., Aghaee, E., Ahmadi, F. & Berijani, S. (2006). Determination of organic compounds in water using dispersive liquid-liquid microextraction. *J. Chromatogr. A*, 1116(1), 1–9. DOI: 10.1016/j.chroma.2006.03.007.
39. Berijani, S., Assadi, Y., Anbia, M., Milani Hosseini, M.R. & Aghaee, E. (2006). Dispersive liquid-liquid microextraction combined with gas chromatography-flame photometric detection: Very simple, rapid and sensitive method for the determination of organophosphorus pesticides in water. *J. Chromatogr. A*, 1123(1), 1–9. DOI: 10.1016/j.chroma.2006.05.010.
40. Tong, S., Liu, S., Wang, H. & Jia, Q. (2014). Recent advances of polymer monolithic columns functionalized with micro/nanomaterials: synthesis and application. *Chromatogr.* 77(1–2), 5–14. DOI: 10.1007/s10337-013-2564-x.
41. Masini, J.C. & Svec, F. (2017). Porous monoliths for on-line sample preparation: a review. *Anal. Chim. Acta*. 964, 24–44. DOI: 10.1016/j.aca.2017.02.002.
42. Lin, F.Y., Chen, W.Y. & Hearn, M.T. (2001). Microcalorimetric studies on the interaction mechanism between proteins and hydrophobic solid surfaces in hydrophobic interaction chromatography: effects of salts, hydrophobicity of the sorbent, and structure of the protein. *Anal. Chem.* 73(16), 3875–3883. DOI: 10.1021/ac0102056.
43. Benavente-García, O., Castillo, J., Marin, F.R., Ortuño, A. & Del Rio, J.A. (1997). Uses and properties of citrus flavonoids. *J. Agric. Food Chem.* 45(12), 4505–4515. DOI: 10.1021/jf970373s.
44. Vinson, J.A., Su, X., Zubik, L. & Bose, P. (2001). Phenol antioxidant quantity and quality in foods: fruits. *J. Agric. Food Chem.* 49(11), 5315–5321. DOI: 10.1021/jf0009293.
45. Vandercook, C.E., & Stephenson, R.G. (1966). Lemon juice composition. Identification of major phenolic compounds and estimation by paper chromatography. *J. Agric. Food Chem.* 14(5), 450–454. DOI: 10.1021/jf60147a003.
46. Prathna, T.C., Chandrasekaran, N., Raichur, A.M. & Mukherjee, A. (2011). Biomimetic synthesis of silver nanoparticles by Citrus limon (lemon) aqueous extract and theoretical prediction of particle size. *Colloids Surf. B: Biointerfaces*, 82(1), 152–159. DOI: 10.1016/j.colsurfb.2010.08.036.
47. Chuag, S.H., Chen, G.H., Chon, H.H., Shen, S.W. & Chen, C.F. (2013). Accelerated colourimetric immunosensing using surface-modified porous monoliths and gold nanoparticles. *Sci. Technol. Adv. Mater.* 14(4), 044403. DOI: 10.1088/1468-6996/14/4/044403.
48. Ganewatta, N. & El Rassi, Z. (2018). Organic polymer-based monolithic stationary phases with incorporated nanostructured materials for HPLC and CEC. *Electrophoresis*, 39(1), 53–66. DOI: 10.1002/elps.201700312.
49. Vergara-Barberán, M., Lerma-García, M.J., Simó-Alfonso, E.F. & Herrero-Martínez, J.M. (2016). Solid-phase extraction based on ground methacrylate monolith modified with gold nanoparticles for isolation of proteins. *Anal. Chim. Acta*, 917, 37–43. DOI: 10.1016/j.aca.2016.02.043.
50. Grzywiński, D., Szumski, M. & Buszewski, B. (2017). Polymer monoliths with silver nanoparticles-cholesterol conjugate as stationary phases for capillary liquid chromatography. *J. Chromatogr. A*, 1526, 93–103. DOI: 10.1016/j.chroma.2017.10.039.
51. Lv, Y., Alejandro, F.M., Fréchet, J.M. & Svec, F. (2012). Preparation of porous polymer monoliths featuring enhanced surface coverage with gold nanoparticles. *J. Chromatogr. A*, 1261, 121–128. DOI: 10.1016/j.chroma.2012.04.007.
52. Sedlacek, O., Kucka, J., Svec, F. & Hruby, M. (2014). Silver-coated monolithic columns for separation in radiopharmaceutical applications. *J. Separ. Sci.* 37(7), 798–802. DOI: 10.1002/jssc.201301325.
53. Acquah, C., Morfo Obeng, E., Agyei, D., Ongkudon, M.C., Moy, C.K.S. & Danquah, M.K. (2017). Nano-doped monolithic materials for molecular separation. *Separations*, 4(1), 2–22. DOI: 10.3390/separations4010002.
54. Vergara-Barberán, M., Lerma-García, M.J., Simó-Alfonso, E.F. & Herrero-Martínez, J.M. (2017). Polymeric sorbents modified with gold and silver nanoparticles for solid-phase extraction of proteins followed by MALDI-TOF analysis. *Microchim. Acta*, 184(6), 1683–1690. DOI: 10.1007/s00604-017-2168-5.